ISBN: 978-3-95450-168-7 doi:10.18429/JACoW-IPAC2015-MOPTY013

CONTROL SYSTEM FOR DC-SRF PHOTO-INJECTOR AT PEKING UNIVERSITY *

L. Feng†, L. Lin, F. Wang, J. Hao, S. Huang S. Quan, K. Liu, B. Zhang
Institute of Heavy Ion Physics, Peking University, Beijing 100871, China

Abstract

A control system has been designed and constructed to full-fill the operation requirement of the DC-SRF photo injector developed at Peking University. The system includes an analog laser phase lock system, FPGA based low level radio frequency (LLRF) control system, PLC based machine protection system, VME based magnet power control, and PC based EPICS IOC. All these systems were integrated to support the stable operation of the DC-SRF photo injector and has shown their robustness. The LLRF system was optimized and tuned for 2K CW/Pulse operation and the stability of amplitude and phase achieves 0.1% and 0.1° respectively.

INTRODUCTION

The DC-SRF [1] photo injector developed at Peking University was designed to generate high repetition rate electron beam in 3-5 MeV range. This injector combines a DC pierce gun and a 3.5-cell superconductor cavity which is capable to operate in both CW and pulse mode. Recently, we've completed the commissioning of the injector [2] and had conducted experiments such as THz coherent wiggler radiation [3] on the platform. The schematic layout of the platform is shown in Fig. 1 and the photo of beamline is shown in Fig. 2.

To make it easier to operate the injector, control of the driver laser, superconductor cavity, beam transport line and other auxiliary systems has to apply. And high level control application such as user interface, data archiver, system-wide interlock was also required.

An EPICS based control system was introduced for this purpose. The remote control of each subsystem was implemented by difference kinds of EPICS IOCs. Control System Studio (CSS) was chose as the OPI tool for its flexibility.

Along with the works on integrating the system, great efforts were also spent on dealing with various of instabilities observed during the experiments. These instabilities were mainly attributed to the phase jitter of laser and RF system. To reduce those instabilities, we've developed a digital Low Level Radio Frequency (LLRF) control system [4] and the laser phase lock system were improved to reduce the relative phase jitter.

SYSTEM DESIGN

The whole system can be divided into five subsystems: injector cryomodule, magnet power supply system, driver laser system, RF control system, and other auxiliary systems such as cooling and vacuum system.

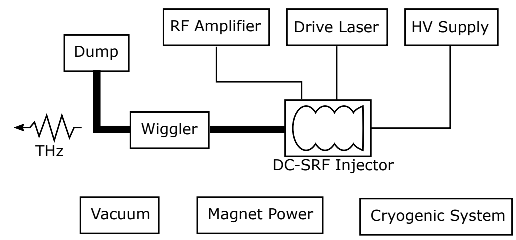

Figure 1: DC-SRF injector THz wiggler radiation experiment layout.

Figure 2: The DC-SRF injector and beamline.

Injector Cryomodule Control

The DC-SRF injector cryomodule is one the main parts of the platform. Its primary function is to maintain 2 K conduction for the super conducting cavity. The cryogenic system that supplies LHe/LN for the cryomodule was constructed by Linde Inc. and Technical Institute of Physics and Chemistry, CAS. The cryogenic system was shipped with a standalone control system and operates independently. Other parts of the injector, however, need controls to ensure the proper operation of it. 16 temperature sensors were installed in the cryomodule. Two Cryocon Model-18 temperature monitors were used to measure those sensors. The measured values can then be transfered to a soft IOC through Ethernet. Because the Model-18 temperature monitor uses just plain text in their communication protocol, it is quite handy to interface them with Asyn/Stream Device module in the IOC.

Besides for the cryogenic system, a high voltage DC power supply is connected to the DC gun of the injector. The high voltage power supply has voltage control input, voltage read

* Work supported by Major State Basic Research Development Program of China (Grant No. 2011CB808302 and 2011CB808304)
† lwfeng@pku.edu.cn

ISBN: 978-3-95450-168-7 doi:10.18429/JACoW-IPAC2015-MOPTY013

back and current read back ports. These signals were interfaced to a Siemens S7-1200 PLC with 0~10 V AI/AO signal module and then transfered to the soft IOC through Ethernet. By connecting the temperature sensors and high voltage power supply to the IOC, all signals from the cryomodule can be monitor and control remotely. And with the use of relational database (RDB) archiver, the historical data can be review if something go wrong with the injector. Fig 3. shows the CSS display for the cryomodule control.

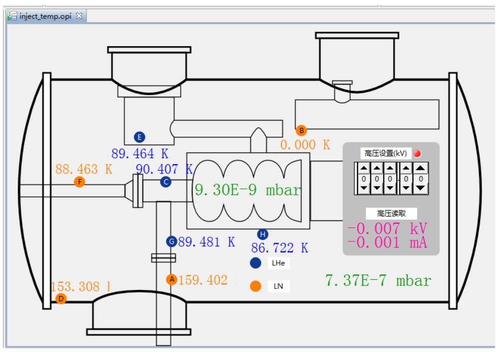

Figure 3: CSS display of the Cryomodule Control.

Magnet Power Supply System

There were two types of magnet power supplies in the electron beam transport line, the main power supplies and the steering coil power supplies. Both supplies were controlled by RS-422/485 serial interfaces and were all install in rack. To increase the IO density, the Acromag IP521 Industry Pack module were chose. Four IP521 module can be installed on one AVME9668 carrier card, and three such carrier card were installed in the 4-slot VME crates. By this way, a total number of 96 serial interfaces were provided by a single IOC.

A MVME6100 VME Single-Board-Computer(SBC) was installed in the VME crates. In the power on procedure, SBC loads the RTEMS embedded OS and EPICS IOC application by network booting through DHCP/BOOTP and TFTP. To control each of the power supply, drivers were derived from asynPortDriver class of Asyn module. And because the RCS signal of each serial channel have to switch fast during each command send/receive, we use direct registers access to the IP521 module instead of making up serial port driver to the OS.

The power controller IOC functions well during the last two year. But lesson was learn here. As more power supplies were installed, the bus speed of VME becomes a bottleneck. Sometimes the SBC is not able to toggle the register bits in time, resulting in communication error. To walk-around this, we have to introduce a global lock in the driver, preventing multi-thread access to the IP521 modules.

Beamline Control

Other devices, such as emittance scanner, insertable screens, faraday cups, and vacuum pumps were also installed in the beamline. These devices were all connected to a Siemens S7-1200 PLC. Fig 4. shows the screen for beamline control.

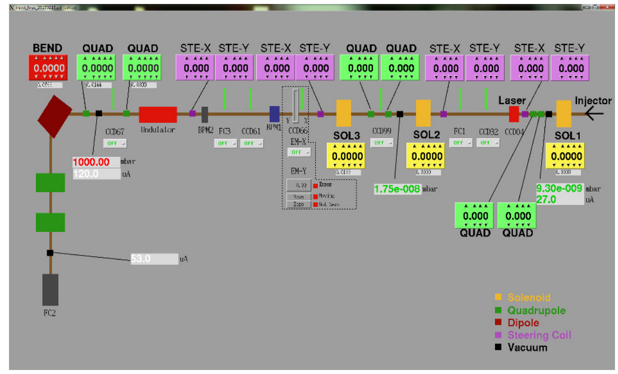

Figure 4: MEDM screen of the beamline control.

Driver Laser System

Driver laser system generates 266 nm picoseconds laser pulse to drive the photocathode. The laser system follows the Seed - Modulate - Amplify - Harmonic Generate scheme. This is similar to the JLab FEL Advanced Drive Laser [5] but instead of second harmonic generation (532 nm), we use the fourth harmonic (266 nm) here. The laser pulse rate of the seed laser is 81.25 MHz. In order to phase-lock the laser pulse to 1.3 GHz microwave, a CLX-1100 controller from Time-Bandwidth Inc. was used. The 1.3 GHz reference signal from Master Oscillator (MO) is first send to a frequency divider and generate the 81.25 MHz reference signal. Then the high speed photo diode (PD) installed in the seed laser chassis was used to generate the laser pulse waveform. These two signals were sent to the phase detector inside CLX-1100 to measure the laser phase error. And then the error signal is sent to a feed-back loop inside CLX-1100 to adjust the piezo and picomotor. By tuning the length of laser cavity, it can then track the reference phase.

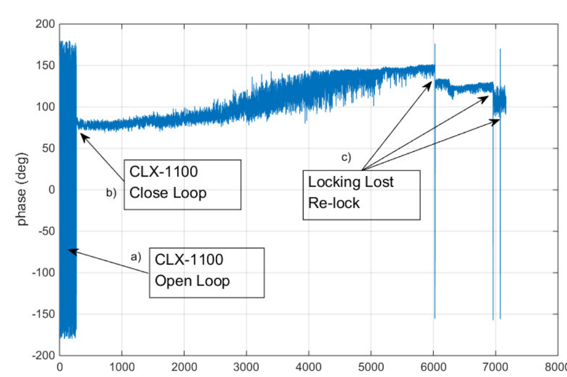

Figure 5: Result of laser phase measurement: a) CLX-1100 open-loop, b) CLX-1100 closed-loop, c) Phase Locking Lost due to picomotor movement.

Phase jitter between acceleration field and laser pulse will greatly degenerate machine performance. According

ISBN: 978-3-95450-168-7 doi:10.18429/JACoW-IPAC2015-MOPTY013

to the CLX-1100 display, the laser phaser jitter is around 1 ps. However, during the experiments, we've observed large beam jitter and slow phase drift that may induced by the laser system. To study the laser performance, we setup a high speed oscilloscope to measure laser phase. Fig 5. shows the measurement result of laser phase. As shown in Fig 5. the phase had drifted 70° in 2 hour.

To deal with this large phase drift, we constructed an external phase lock loop for the laser system. This loop takes 16th harmonic of the PD signal and then mix it with the MO. The mixer output is then related to their phase error:

$$V_{ref} \cdot V_{PD} \cdot sin(\theta_{ref} - \theta_{PD})$$

Here we selected the operation point of both amplifiers to well above their P1d, thus lower the influence of signal amplitude change and maximize the mixer gain. As shown in Fig 6., the phase error signal is filtered and then sampled by a NI USB-6343 DAQ card. A Labview program runs on the control PC to calculate phase drift of the laser signal. Then it apply a 0~10 V signal to the delay input port of CLX-1100 to correct the phase drift error. Fig 6. shows the Labview program that controls the external loop. Note that the system starts in closed-loop status, the phase(red curve) stays stable even when after two locking lose event. Then in the middle of the curve, we deliberately disable the feed-back loop, and the laser phase starts to drift.

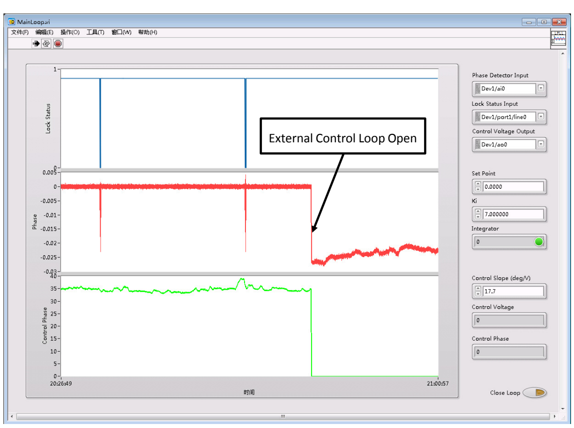

Figure 6: Control Screen of External Laser Phase Lock. Blue curve: CLX-1100 Lock status. Red curve: Phase error signal. Green curve: phase correction signal

RF Control System

We built a digital LLRF system to control the SRF injector cavity. The LLRF amplitude and phase stability achieves 0.1% and 0.1° respectively (Shown in Fig 7.). Fig 8. shows a running LLRF control UI written in python.

CONCLUSIONS

In this article, we briefly introduced the structure of Peking University DC-SRF injector control system. This system achieved its design goal and performs well. Improvements made to the laser and RF control also show a good result too.

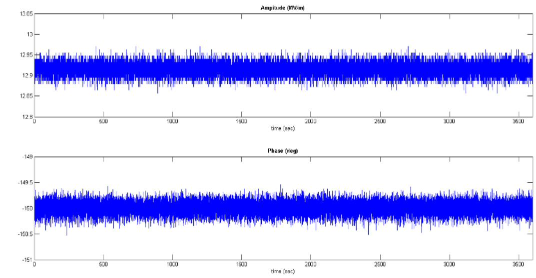

Figure 7: Cavity amplitude (up) and phase (below) plot at 12.9MV/m without beam-loaded.

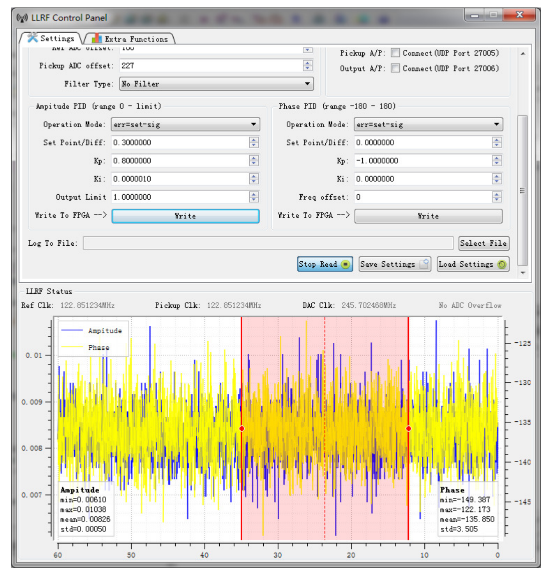

Figure 8: Control Interface of LLRF.

REFERENCES

[1] J. Hao et al., "3.5-cell Superconducting Cavity for DC-SRF Photoinjector at Peking University", SRF2009, Berlin, Gremany, TUPPO013.

[2] K. Liu et al., "Commissioning and Operation of DC-SRF Injector", SRF2013, Paris, France, MOIOB04.

[3] S.L. Huang et al., "Coherent Wiggler Radiation of Picosecond CW Electron Beam Produced by DC-SRF Photoinjector" IPAC2013, Shanghai, China, MOPEA038.

[4] H. Zhang et al., "LLRF Control System for PKU DC-SC Photocathode Injector", IPAC2011, San Sebastián, Spain, MOPC097.

[5] F. G. Wilson et al., "Characterization and Suppression of the Electromagnetic Interference Induced Phase Shift in the JLab FEL Photo – Injector Advanced Drive Laser System", PAC2011, New York, USA, THP225.